

Enhanced single-photon emission from a quantum dot in a micropost microcavity

Jelena Vučković, David Fattal, Charles Santori, Glenn S. Solomon and
Yoshihisa Yamamoto

Quantum Entanglement Project, ICORP, JST
Ginzton Laboratory, Stanford University, Stanford CA 94305

November 16, 2018

Abstract

We demonstrate a single-photon source based on a quantum dot in a micropost microcavity that exhibits a large Purcell factor together with a small multi-photon probability. For a quantum dot on resonance with the cavity, the spontaneous emission rate is increased by a factor of five, while the probability to emit two or more photons in the same pulse is reduced to 2% compared to a Poisson-distributed source of the same intensity. In addition to the small multi-photon probability, such a strong Purcell effect is important in a single-photon source for improving the photon outcoupling efficiency and the single-photon generation rate, and for bringing the emitted photon pulses closer to the Fourier transform limit.

Generation of single photons at a well defined timing or clock is crucial for practical implementation of quantum key distribution (QKD) [1], as well as for quantum computation [2] and networking based on photonic qubits [3, 4]. Three different criteria are taken into account when evaluating the quality of a single-photon source: high efficiency, small multi-photon probability (measured by the second-order coherence function $g^{(2)}(0)$), and quantum indistinguishability. For example, high efficiency and small $g^{(2)}(0)$ are required, but quantum indistinguishability is not necessary for BB84 QKD [5]. On the other hand, for almost all other applications in quantum information systems we need photons that are indistinguishable and thus produce multi-photon interference.

One of the popular approaches to generation of single photons is based on a pulsed excitation of a quantum dot (QD) combined with spectral filtering [6, 7, 8, 9]. Although a single quantum dot by itself can be used to generate single photons [6], the efficiency of such a system is poor, as the majority of emitted photons are lost in the substrate. In addition, the radiative lifetime can be as long as 1 ns, which is greater than the dephasing time estimated to be ~ 0.9 ns at 4K [10]. Emitted

photons are unlikely to be indistinguishable, with coherence lengths shorter than the radiative limit (Fourier transform limit). Finally, the single-photon generation rate is low, as determined by the long excitonic lifetime. Microcavities can help in correcting all of these deficiencies [11, 8, 7]. The radiative lifetime of an emitter on resonance with the cavity can be decreased significantly below the dephasing time, bringing the emitted photon pulses closer to the Fourier transform limit. Moreover, the spontaneous emission rate can be enhanced, and a large fraction of spontaneously emitted photons can be coupled into a single cavity mode, thereby increasing the outcoupling efficiency. By employing a QD in a micropost microcavity, our group has recently demonstrated efficiencies close to 40% [12]. We have also proved that consecutive photons emitted from such a source are largely indistinguishable, with a mean wave-packet overlap as large as 0.81 [13]. In this article, we demonstrate an improved single-photon source based on a quantum dot in a micropost microcavity that exhibits a large Purcell factor ($F_p=5$) together with a small multi-photon probability ($g^2(0)=2\%$).

Our single-photon source consists of a self-assembled InAs QD embedded in the middle of a GaAs spacer in a distributed Bragg reflector (DBR) micropost microcavity. The GaAs spacer is approximately one optical wavelength thick (274 nm), and sandwiched between twelve DBR mirror pairs on top, and thirty DBR mirror pairs on bottom. Each DBR pair consists of a 68.6 nm thick GaAs and a 81.4 nm thick AlAs layer (both layers are approximately quarter-wavelength thick). The advantages of microposts relative to other microcavities are that the light escapes normal to the sample, in a single-lobed Gaussian-like pattern, and that it is relatively straightforward to isolate a single QD in them. The micropost structures (shown in Fig. 1) were constructed by a combination of molecular-beam epitaxy (MBE) and chemically assisted ion beam etching (CAIBE). MBE was used to grow a wafer consisting of DBR mirrors and a GaAs spacer with embedded self-assembled QDs. Microposts with diameters ranging from $0.3 \mu\text{m}$ to $5 \mu\text{m}$ and heights of $5 \mu\text{m}$ were fabricated in a random distribution by

CAIBE, with Ar^+ ions and Cl_2 gas, and using sapphire (Al_2O_3) dust particles as etch masks. Sapphire was chosen as a mask because of its chemical stability and hardness, which enabled larger etch depths than other mask-materials. Unfortunately, these same properties impede its removal from the tops of the structures, without endangering the microposts [14]. The presence of sapphire on top of the structures decreases their quality factors and consequently reduces outcoupling efficiencies. This can be confirmed theoretically by the Finite Difference Time Domain (FDTD) calculation of the Q-factor of the fundamental HE_{11} mode (whose field pattern is also shown in Fig. 1) in a micropost with and without sapphire on top. The details of the FDTD method can be found in our earlier publication [15]; the FDTD unit cell size used in this case is 5 nm. We assume that the DBR layers of the simulated post have the same parameters as in the experimentally studied structures, that the post has perfectly straight walls, diameter of $0.5 \mu\text{m}$, and that refractive indices of GaAs, AlAs, and Al_2O_3 are 3.5, 2.9, and 1.75, respectively. Without sapphire, the Q-factor of the HE_{11} mode is 2600 and its wavelength is 882 nm; with $0.5 \mu\text{m}$ thick sapphire disk on top of the post (with diameter equal to that of the post), the Q-factor drops to 1400, while the mode wavelength remains unchanged. Due to the irregular shapes of the fabricated posts, the HE_{11} mode is typically polarization-nondegenerate, and many microposts have only one or two QDs on resonance with this fundamental mode.

In our experimental setup, the sample with microposts is placed in a liquid He cryostat. The microposts are excited from a steep angle by Ti:sapphire laser pulses, 3 ps in duration, with a 76 MHz repetition rate, and resonant with higher-level confined states of a QD. With resonant excitation, the favored absorption of a single electron-hole pair is expected, and no carriers are created in the vicinity of the QD, suppressing emission wavelength drift due to charge fluctuations. The emission from the QD is collected normal to the sample surface, and then directed towards a streak camera preceded by a spectrometer, for time-resolved photoluminescence measurements. The spectral resolution of the system is 0.1 nm, together with a time resolution of 25 ps. For photon correlation measurements, the collected emission is first spectrally filtered with bandwidth of 0.1 nm and then directed towards a Hanbury Brown and Twiss-type (HBT) setup. In the HBT setup, photon counters are placed at both outputs of a non-polarizing beamsplitter for detection. The electronic signals from the counters are sent to a time-to-amplitude converter followed by a multi-channel analyzer computer card, which generates a histogram of the relative delay time $\tau = t_2 - t_1$ between a photon detection at one counter (t_2) and the other (t_1). For the detailed description of the setup, please refer to [6].

We performed lifetime and $g^{(2)}$ measurements on a QD chosen for its bright emission under resonant excitation. Tuning of the sample temperature was used to tune the emission wavelength relative to the cavity res-

onance [16]. In this particular case, the dot emission wavelength was tuned away from the cavity resonance by increasing the sample temperature from 6 K to 40 K [17]. Fig. 2 (bottom) shows the time-resolved photoluminescence of an emission line on- and off-resonance with the cavity mode. The decay lifetime differs by a factor of five for these two cases. The decay rate for this emission line as a function of the absolute value of its detuning from the cavity resonance ($|\lambda_{QD} - \lambda_c|$) is plotted with circles in the top-right plot of Fig. 2. The solid line corresponds to the Lorentzian fit to the experimental data [11], and a good match is observed between our experiment and the theoretically predicted behavior. The fitting parameters are the linewidth, maximum and minimum of the Lorentzian, while it is assumed that its central wavelength is equal to λ_c , the cavity resonance wavelength. λ_c and the quality factor ($Q = 1270$) are determined from the photoluminescence intensity taken at high pump powers (see the top-left plot of Fig. 2). The cavity resonance wavelength red-shifts by roughly 0.3 nm with increasing temperature in the studied range, and this shift is included in plotting the data. Up to fivefold spontaneous emission rate enhancement (Purcell factor F_p) is observed for the dot coupled to a cavity, as opposed to the dot off-resonance (top-right plot of Figure 2).

The theoretical limit of the Q-factor of the studied microposts is 4000, which is the value calculated for a planar cavity (before etching) without any absorption losses and inaccuracies in the growth of DBR layers. The maximum Q-factor of a micropost with a finite diameter has to be below this limit, due to the additional loss mechanisms in the transverse directions [15] and the presence of sapphire dust particles, as discussed above. According to the detailed theoretical treatment of the QD micropost device [15, 18], the cavity Q-factor and Purcell factor can be much larger ($Q \sim 10000$ and $F_p \sim 100$) for optimized cavity designs with 15 and 30 DBR pairs on top and bottom, respectively, perfectly straight cavity walls, and a QD located at the cavity center.

A photon-correlation measurement for this same dot on resonance with the cavity is shown in Fig. 3. The histogram is generated using the described HBT setup. The distance between peaks is 13 ns, corresponding to the repetition period of pulses from the Ti:sapphire laser. The decrease in the height of the side peaks as $|\tau|$ increases indicates the dot blinking behavior generally observed under resonant excitation, and can be approximated with a double-sided exponential [6]. The vanishing central peak (at $\tau=0$) indicates a strong antibunching and a large suppression of multi-photon pulses. The probability of generating two and more photons for the same laser pulse compared to a Poisson-distributed source of the same intensity ($g^2(0)$) is estimated from the ratio of the areas of the central peak and the peaks at $|\tau| \rightarrow \infty$. Each area is calculated by integrating all the counts within the integration window centered at the peak and without subtracting any background counts.

The area of the peak at $|\tau| \rightarrow \infty$ is estimated from the decaying exponential fit to the heights of the side peaks. $g^2(0)$ is estimated to be equal to 2% for an integration window of 4 ns. The integration window is chosen so that the contribution of the peak tails outside it to the peak area can be neglected (it is below 1%). The width of the histogram peaks is determined by the photon counter timing resolution (0.3 ns) and the excitonic lifetime [6]. Owing to the strong Purcell effect (excitonic lifetime below 0.2 ns), this small multiphoton probability should be preserved even for the repetition period much smaller than 13 ns (e.g., 2 ns). If the integration window is reduced to 1 ns, $g^2(0)$ drops to 1%. Depending on the application of the photon-source, a different definition of the two-photon probability may be necessary. For example, in the interference experiment with two consecutive photons emitted from a dot, the relevant parameter is the probability to emit two photons in the same pulse, as opposed to the probability to emit one photon in each of the two consecutive pulses [13]. This parameter, which we denote as g , is calculated from the ratio of the area of the central peak to the area of the nearest side peak, and is equal to 0.9% for the integration window of 4 ns. The difference between g and $g^2(0)$ is a result of the blinking behavior of the dot.

In summary, we have studied the effect of a microcavity on single photons emitted from a QD, and have demonstrated an improved single-photon source that exhibits a large Purcell factor ($F_p=5$) together with a small multi-photon probability ($g^2(0)=2\%$). In addition to a small multi-photon probability, such a strong Purcell effect is important in a single-photon source for improving the photon outcoupling efficiency and the single-photon generation rate, and for bringing the emitted photon pulses closer to the Fourier transform limit.

Acknowledgement

This work is partially supported by MURI UCLA/0160-G-BC575. The authors would like to thank A. Scherer and T. Yoshie from Caltech for providing access to CAIBE and for helping with fabrication.

Jelena Vučković is with the Department of Electrical Engineering, Stanford University, Stanford, CA 94305. E-mail: jela@stanford.edu. Charles Santori is also at the IIS, University of Tokyo, Tokyo, Japan. Glenn S. Solomon is also at the SSPL, Stanford University, Stanford, CA 94305. Yoshihisa Yamamoto is also at NTT Basic Research Labs, Atsugishi, Japan.

References

- [1] C. H. Bennet and G. Brassard. *Proceedings of the IEEE International Conference on Computers, Systems and Signal Processing*. IEEE, Bangalore, India, 1984.
- [2] E. Knill, R. Laflamme, and G. J. Milburn. A scheme for efficient quantum computation with linear optics. *Nature*, 409:46–52, 2001.
- [3] J.I. Cirac, P. Zoller, H.J. Kimble, and H. Mabuchi. Quantum state transfer and entanglement distribution among distant nodes in a quantum network. *Physical Review Letters*, 78:3221, 1997.
- [4] L.M. Duan, M.D. Lukin, J.I. Cirac, and P. Zoller. Long-distance quantum communication with atomic ensembles and linear optics. *Nature*, 414:413–418, 2001.
- [5] Edo Waks, Charles Santori, and Yoshihisa Yamamoto. Security aspects of quantum key distribution with sub-Poissonian light. *Physical Review A*, 66:042315, October 2002.
- [6] C. Santori, M. Pelton, G. Solomon, Y. Dale, and Y. Yamamoto. Triggered single photons from a quantum dot. *Physical Review Letters*, 86(8):1502–1505, 2001.
- [7] P. Michler, A. Kiraz, C. Becher, W. V. Schoenfeld, P. M. Petroff, L. Zhang, E. Hu, and A. Imamoglu. A quantum dot single-photon turnstile device. *Science*, 290:2282–2285, 2000.
- [8] E. Moreau, I. Robert, J. M. Gérard, I. Abram, L. Manin, and V. Thierry-Mieg. Single-mode solid-state single photon source based on isolated quantum dots in pillar microcavities. *Applied Physics Letters*, 79(18):2865–2867, 2001.
- [9] V. Zwiller, H. Blom, P. Jonsson, N. Panev, S. Jeppesen, T. Tsegaye, E. Goobar, M. E. Pistol, L. Samuelson, and G. Bjork. Single quantum dots emit single photons at a time: antibunching experiments. *Applied Physics Letters*, 78:2476–2478, 2001.
- [10] M. Bayer and A. Forchel. Temperature dependence of the exciton homogeneous linewidth in InGaAs/GaAs self-assembled quantum dots. *Physical Review B*, 65:041308, 2002.
- [11] J. M. Gérard, B. Sermage, B. Gayral, B. Legrand, E. Costard, and V. Thierry-Mieg. Enhanced spontaneous emission by quantum boxes in a monolithic optical microcavity. *Physical Review Letters*, 81:1110–1113, 1998.
- [12] M. Pelton, C. Santori, J. Vučković, B. Zhang, G. S. Solomon, J. Plant, and Y. Yamamoto. An efficient source of single photons: a single quantum dot in a micropost microcavit. *Physical Review Letters*, 89:233602, 2002.
- [13] C. Santori, D. Fattal, J. Vučković, G. Solomon, and Y. Yamamoto. Indistinguishable photons from a single-photon device. *Nature*, 419(6907):594–597, October 2002.

- [14] P. Levy, M. Bianconi, and L. Correr. Wet etching of Al_2O_3 for selective patterning of microstructures using Ar^+ ion implantation and H_3PO_4 . *Journal of the Electrochemical Society*, 145:344, 1998.
- [15] J. Vučković, M. Pelton, A. Scherer, and Y. Yamamoto. Optimization of three-dimensional micropost microcavities for cavity quantum electrodynamics. *Physical Review A*, 66:023808, August 2002.
- [16] A. Kiraz, P. Michler, C. Becher, B. Gayral, A. Imamoglu, L. Zhang, E. Hu, W. V. Schoenfeld, and P. M. Petroff. Cavity-quantum electrodynamics using a single InAs quantum dot in a microdisk structure. *Applied Physics Letters*, 78:3932–3934, 2001.
- [17] This QD is almost exactly on resonance with the cavity at low temperature, so by heating the sample and increasing the QD emission wavelength, one also increases the detuning from the cavity resonance and the radiative lifetime. The opposite process is observed if the QD emission wavelength is initially smaller than the cavity resonance. In addition to a good correspondence between the cavity resonance linewidth and the Lorentzian linewidth, these processes indicate that the cavity QED has a dominant effect on the radiative lifetime.
- [18] M. Pelton, J. Vučković, G. S. Solomon, A. Scherer, and Y. Yamamoto. Three-dimensionally confined modes in micropost microcavities: Quality factors and Purcell factors. *IEEE Journal of Quantum Electronics*, 38(2):170–177, 2002.

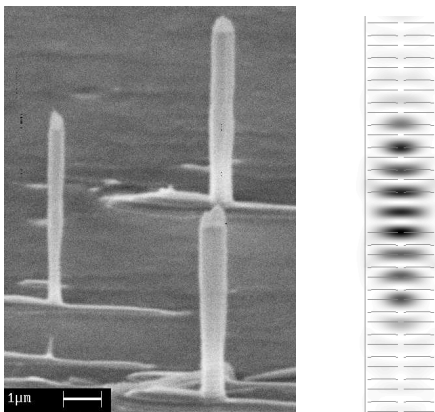


Figure 1: Left: Scanning electron micrograph showing a fabricated array of microposts. Remaining sapphire dust (used as etch mask) is visible at the top of the structures. Right: Simulated electric field intensity of the fundamental HE_{11} mode in a cavity.

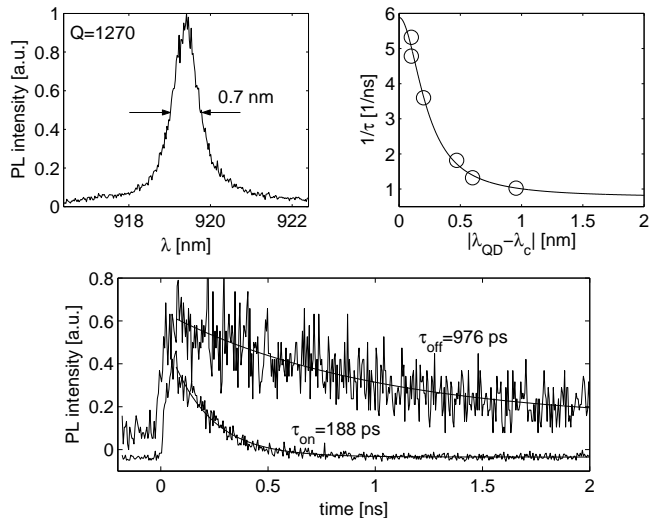


Figure 2: Top-left: Background emission filtered by the cavity. Top-right: Decay rate of the emission line as a function of the absolute value of its detuning from the cavity resonance ($|\lambda_{\text{QD}} - \lambda_c|$). The dot emission wavelength was tuned by changing the sample temperature within the 6 K - 40 K range. Bottom: time-dependent photoluminescence from the emission line on-resonance with the cavity, as opposed to this same emission line off-resonance.

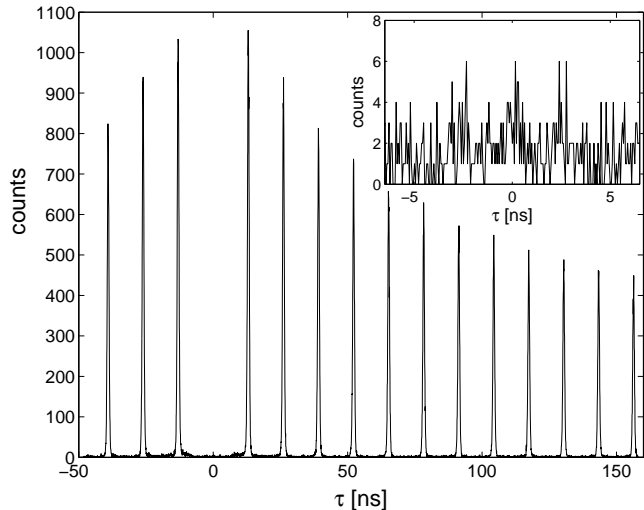


Figure 3: Photon correlation histogram for a QD on resonance with the cavity (the lifetime of this dot is shown in Fig. 2), under pulsed, resonant excitation. The inset depicts the magnified central portion (from $\tau = -6.5$ ns to 6.5 ns) of the histogram. The missing central peak (at $\tau = 0$) indicates a large suppression of multi-photon pulses.